

Ca²⁺ Uniporter

Transporter

(Version 2)

In Mitochondria

Author(s): Ranjan K. Dash, Feng Qi and Daniel A. Beard
 Biotechnology and Bioengineering Center, Department of Physiology
 Medical College of Wisconsin

Contact: dbeard@mcw.edu

Publication: Dash, RK , Qi, Feng and Beard, DA. A Biophysically-Based Mathematical Model for the Kinetics of Mitochondrial [Ca²⁺] Uniporter. (Manuscript in Review), 2008.

Function

Ca²⁺ is taken up in energized mitochondria via the Ca²⁺ uniporter (CU). It is driven by the electrochemical gradient of Ca²⁺ across the inner mitochondrial membrane (IMM). It is also influenced by the kinetics of Ca²⁺ binding to the CU. CU plays a major role in mitochondrial function or dysfunction by regulating the dynamics of mitochondrial [Ca²⁺].

Mechanism

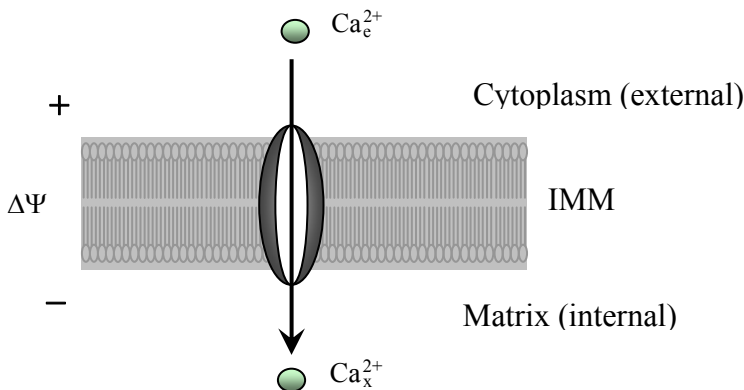


Figure 1a: General schematic of the Ca²⁺ transport via the Ca²⁺ uniporter. The arrow shows the direction of net flux. The scheme also shows the sign convention for membrane potential.

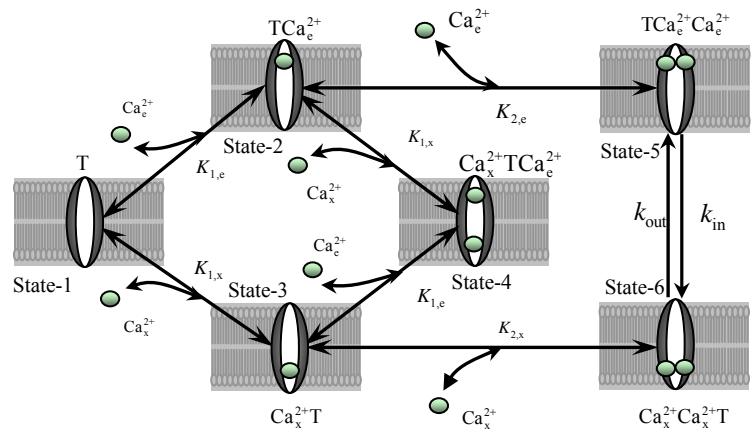
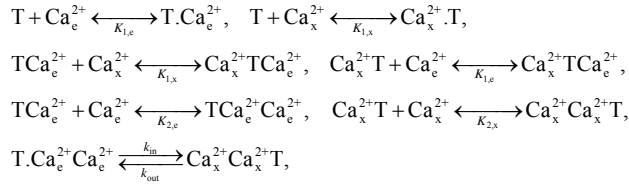


Figure 1b: The proposed 6-states kinetic mechanism of Ca²⁺ transport into mitochondria through the Ca²⁺ uniporter. The uniporter is assumed to have two binding sites for Ca²⁺ and the Ca²⁺ is assumed to bind to the uniporter from either side of the inner mitochondrial membrane (IMM). The ionized free Ca²⁺ from the cytoplasmic side of the IMM cooperatively binds to the unbound uniporter (T) (state-1) in two steps to form the complex TCa_e²⁺Ca_e²⁺ (state-5) which then undergo conformational changes (or flips upside down) to form the complex Ca_x²⁺Ca_x²⁺T (state-6). The complex Ca_x²⁺Ca_x²⁺T in the matrix side of the IMM

goes through the reverse process where it dissociates in two steps to form the unbound uniporter (T) and ionized free Ca^{2+} . The model also assumes the cross-interactions between the uniporter, external Ca^{2+} , and internal Ca^{2+} to form the intermediate complex $\text{Ca}_x^{2+}\text{TCa}_e^{2+}$ (dead end, state-4). The other two states of the uniporter are the bound uniporter TCa_e^{2+} (state-2) and TCa_x^{2+} (state-3). ($K_{1,e}$, $K_{1,x}$) and ($K_{2,e}$, $K_{2,x}$) are the two pairs of dissociation (binding) constants for the two step uniporter binding reactions with the external and internal Ca^{2+} . The transport of Ca^{2+} via the Ca^{2+} uniporter is limited by the rate constants k_{in} and k_{out} which are dependent on the membrane potential $\Delta\Psi$.

Equations

The reactions for the uniporter- Ca^{2+} binding and the reaction for the conformational change of the ternary uniporter- 2Ca^{2+} binding complex can be written as



Under the quasi-steady state, rapid equilibrium binding assumptions, we have the following relationships between the various states of the uniporter:

$$\begin{aligned} [\text{TCa}_e^{2+}] &= \frac{[\text{Ca}_e^{2+}]_e}{K_{1,e}} [\text{T}], & [\text{Ca}_x^{2+} \text{T}] &= \frac{[\text{Ca}_x^{2+}]_x}{K_{1,x}} [\text{T}], & [\text{TCa}_e^{2+} \text{Ca}_e^{2+}] &= \frac{[\text{Ca}_e^{2+}]_e^2}{K_{1,e} K_{2,e}} [\text{T}], \\ [\text{Ca}_x^{2+} \text{Ca}_x^{2+} \text{T}] &= \frac{[\text{Ca}_x^{2+}]_x^2}{K_{1,x} K_{2,x}} [\text{T}], & [\text{Ca}_x^{2+} \text{TCa}_e^{2+}] &= \frac{[\text{Ca}_x^{2+}]_x [\text{Ca}_e^{2+}]_e}{K_{1,x} K_{1,e}} [\text{T}], \end{aligned}$$

where the concentrations of free and Ca^{2+} -bound uniporter states are expressed with respect to the

mitochondrial matrix volume; $[\text{Ca}^{2+}]_e$ and $[\text{Ca}^{2+}]_x$ denote the extra-mitochondrial and matrix concentrations of Ca^{2+} ; $K_{1,e}$, $K_{1,x}$, $K_{2,e}$, and $K_{2,x}$ are in the units of concentration (molar).

Since the total uniporter concentration $[\text{T}]_{\text{tot}}$ is constant, we have by mass conservation

$$[\text{T}] + [\text{Ca}_e^{2+} \text{T}] + [\text{TCa}_x^{2+}] + [\text{Ca}_x^{2+} \text{TCa}_e^{2+}] + [\text{Ca}_e^{2+} \text{Ca}_e^{2+} \text{T}] + [\text{TCa}_x^{2+} \text{Ca}_x^{2+}] = [\text{T}]_{\text{tot}}.$$

By combining the above equations, we can say

$$[\text{T}] = [\text{T}]_{\text{tot}} / D,$$

where,

$$D = 1 + \frac{[\text{Ca}_e^{2+}]_e}{K_{1,e}} + \frac{[\text{Ca}_x^{2+}]_x}{K_{1,x}} + \frac{[\text{Ca}_e^{2+}]_e [\text{Ca}_x^{2+}]_x}{K_{1,e} K_{1,x}} + \frac{[\text{Ca}_e^{2+}]_e^2}{K_{1,e} K_{2,e}} + \frac{[\text{Ca}_x^{2+}]_x^2}{K_{1,x} K_{2,x}}.$$

The flux through the uniporter can be expressed as

$$J_{\text{uni}} = k_{in} [\text{Ca}_e^{2+} \text{Ca}_e^{2+} \text{T}] - k_{out} [\text{TCa}_x^{2+} \text{Ca}_x^{2+}] = \frac{[\text{T}]_{\text{tot}}}{D} \left(k_{in} \frac{[\text{Ca}_e^{2+}]_e^2}{K_{1,e} K_{2,e}} - k_{out} \frac{[\text{Ca}_x^{2+}]_x^2}{K_{1,x} K_{2,x}} \right).$$

which is characterized by six unknown parameters.

Model 1

We can reduce the number of parameters by two by making the approximation that the first binding constants $K_{1,e}$ and $K_{1,x}$ are to be large compared to the second binding constants $K_{2,e}$ and $K_{2,x}$ with the constraints that $K_{1,e} \cdot K_{2,e} = K_e^2$ and $K_{1,x} \cdot K_{2,x} = K_x^2$ are finite (cooperative binding). These approximations can be valid under the assumptions $K_{1,e} \gg 1$, $K_{1,x} \gg 1$, $K_{2,e} \ll 1$ and $K_{2,x} \ll 1$. In this case, the concentrations of TCa_e^{2+} , $\text{Ca}_x^{2+} \text{T}$ and $\text{Ca}_x^{2+} \text{TCa}_e^{2+}$ can be considered negligible compared to the concentrations of the other binding states of the uniporter. The flux expression can be reduced to

$$J_{\text{Uni}} = \frac{[T]_{\text{tot}}}{D_1} \left(k_{\text{in}} \frac{[\text{Ca}^{2+}]_e^2}{K_e^2} - k_{\text{out}} \frac{[\text{Ca}^{2+}]_x^2}{K_x^2} \right),$$

where

$$D_1 = 1 + \frac{[\text{Ca}^{2+}]_e^2}{K_e^2} + \frac{[\text{Ca}^{2+}]_x^2}{K_x^2}.$$

At equilibrium conditions, the kinetic parameters K_e , K_x , k_{in} and k_{out} can be further constrained by the following equilibrium relationships:

$$\frac{k_{\text{in}} \cdot K_x^2}{k_{\text{out}} \cdot K_e^2} = \frac{[\text{Ca}^{2+}]_{x,\text{eq}}^2}{[\text{Ca}^{2+}]_{e,\text{eq}}^2} = K_{\text{eq}}.$$

By taking into account the membrane potential $\Delta\Psi$ dependencies (see Figure 2), we can define the kinetic parameters as follows based on Eyring's free-energy barrier theory:

$$\begin{aligned} K_{\text{eq}} &= \exp(2\Delta\Phi), \quad \Delta\Phi = Z_{\text{Ca}} F \Delta\Psi / RT, \\ K_e &= K_e^0 \exp(-\alpha_e \Delta\Phi), \\ K_x &= K_x^0 \exp(+\alpha_x \Delta\Phi), \\ k_{\text{in}} &= k_{\text{in}}^0 \exp(+2\beta_e \Delta\Phi), \text{ and} \\ k_{\text{out}} &= k_{\text{out}}^0 \exp(-2\beta_x \Delta\Phi), \end{aligned}$$

where K_e^0 and K_x^0 are the values of the binding constants in the absence of an electric field ($\Delta\Psi=0$ mV) and

$$k_{\text{in}}^0 = \frac{k_B T}{h} \exp(-\Delta G_{\text{in}}^0 / RT) \quad \text{and} \quad k_{\text{out}}^0 = \frac{k_B T}{h} \exp(-\Delta G_{\text{out}}^0 / RT)$$

are the forward and reverse rate constants in the absence of electric field.

By substituting the parameters into the flux expression, we derive the final flux expression

$$J_{\text{Uni}} = X_{\text{Uni}} \frac{([\text{Ca}^{2+}]_e^2 \exp(+\Delta\Phi) - [\text{Ca}^{2+}]_x^2 \exp(-\Delta\Phi)) \exp((2\alpha_e + 2\beta_e - 1)\Delta\Phi)}{(K_x^{02} + (K_x^0 / K_e^0)^2 [\text{Ca}^{2+}]_e^2 \exp(2\alpha_e \Delta\Phi) + [\text{Ca}^{2+}]_x^2 \exp(-2\alpha_x \Delta\Phi))},$$

where $X_{\text{Uni}} = [T]_{\text{tot}} k_{\text{out}}^0$.

Model 2

We can also reduce the number of parameters by two by making the assumption that the first binding constants $K_{1,e}$ and $K_{1,x}$ are to be equal to the second binding constants $K_{2,e}$ and $K_{2,x}$, respectively; in other words, $K_{1,e} = K_{2,e} = K_e$ and $K_{1,x} = K_{2,x} = K_x$. In this case, the flux expression can be reduced to

$$J_{\text{Uni}} = \frac{[T]_{\text{tot}}}{D_2} \left(k_{\text{in}} \frac{[\text{Ca}^{2+}]_e^2}{K_e^2} - k_{\text{out}} \frac{[\text{Ca}^{2+}]_x^2}{K_x^2} \right),$$

where

$$D_2 = 1 + \frac{[\text{Ca}^{2+}]_e}{K_e} + \frac{[\text{Ca}^{2+}]_x}{K_x} + \frac{[\text{Ca}^{2+}]_e [\text{Ca}^{2+}]_x}{K_e K_x} + \frac{[\text{Ca}^{2+}]_e^2}{K_e^2} + \frac{[\text{Ca}^{2+}]_x^2}{K_x^2}.$$

By substituting the same parameters as before into the flux expression, we drive the final flux expression

$$J_{\text{Uni}} = X_{\text{Uni}} \frac{([\text{Ca}^{2+}]_e^2 \exp(+\Delta\Phi) - [\text{Ca}^{2+}]_x^2 \exp(-\Delta\Phi)) \exp((2\alpha_e + 2\beta_e - 1)\Delta\Phi)}{\left(K_x^{02} + (K_x^0 / K_e^0) [\text{Ca}^{2+}]_e \exp(\alpha_e \Delta\Phi) + K_x^0 [\text{Ca}^{2+}]_x \exp(-\alpha_x \Delta\Phi) \right. \\ \left. + (K_x^0 / K_e^0) [\text{Ca}^{2+}]_e [\text{Ca}^{2+}]_x \exp((\alpha_e - \alpha_x) \Delta\Phi) \right. \\ \left. + (K_x^0 / K_e^0)^2 [\text{Ca}^{2+}]_e^2 \exp(2\alpha_e \Delta\Phi) + [\text{Ca}^{2+}]_x^2 \exp(-2\alpha_x \Delta\Phi) \right)}$$

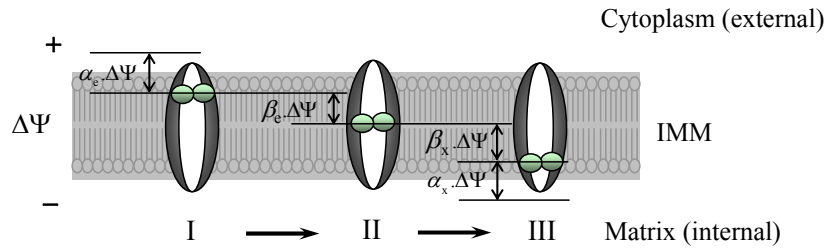
where $X_{\text{Uni}} = [T]_{\text{tot}} k_{\text{out}}^0$.

Parameters

Parameter	Model 1		Model 2		References
	Case 1 ($K_e^0 = K_x^0$)	Case 2 ($K_e^0 \neq K_x^0$)	Case 1 ($K_e^0 = K_x^0$)	Case 2 ($K_e^0 \neq K_x^0$)	
k_{in}^0 (nmol/mg/sec)	49.55	0.55	35.0	0.5	[3]
	0.32	3.55×10^{-3}	0.39	5.56×10^{-3}	[1]
	0.354	3.986×10^{-3}	0.4375	6.76×10^{-3}	[4]
k_{out}^0 (nmol/mg/sec)	49.55	0.0085	35.0	0.028	[3]
	0.32	54.84×10^{-6}	0.39	311.1×10^{-6}	[1]
	0.354	61.59×10^{-6}	0.4375	378.4×10^{-6}	[4]
K_e^0 (M)	48×10^{-6}	15×10^{-6}	40×10^{-6}	12×10^{-6}	[3]
	48×10^{-6}	15×10^{-6}	40×10^{-6}	12×10^{-6}	[1]
	90×10^{-6}	78.75×10^{-6}	75×10^{-6}	63×10^{-6}	[4]
K_x^0 (M)	48×10^{-6}	1.865×10^{-6}	40×10^{-6}	2.84×10^{-6}	[3]
	48×10^{-6}	1.865×10^{-6}	40×10^{-6}	2.84×10^{-6}	[1]
	90×10^{-6}	9.79×10^{-6}	75×10^{-6}	14.91×10^{-6}	[4]
α_e (unitless)	0.0	0.0	0.0	0.0	[3],[1],[4]
α_x (unitless)	0.038	-0.214	0.0375	-0.239	[3],[1],[4]
β_e (unitless)	0.112	0.264	0.1125	0.259	[3],[1],[4]
β_x (unitless)	0.85	0.95	0.85	0.98	[3],[1],[4]
Standard physiochemical/thermodynamic parameters used in the model					
RT	Gas constant times temperature		2.5775	kJ mol^{-1}	
F	Faraday's constant		0.096484	$\text{kJ mol}^{-1} \text{mV}^{-1}$	
Z_{Ca}	Valence of Ca^{2+}		2	unitless	

Table 1: Parameter estimates for both models under the assumptions $K_e^0 = K_x^0$ and $K_e^0 \neq K_x^0$. The constraints $(k_{in}^0 / k_{out}^0) \cdot (K_x^0 / K_e^0)^2 = 1$ and $\alpha_e + \alpha_x + \beta_e + \beta_x = 1$ were used to reduce the number of final parameters. In other words, only six parameters were estimated for each case, and the final two were calculated based upon the above constraints.

A



B

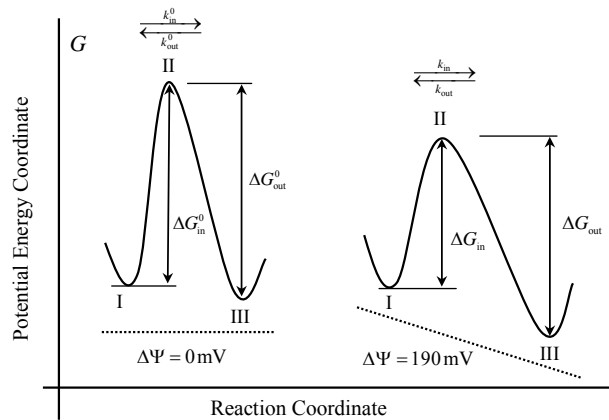
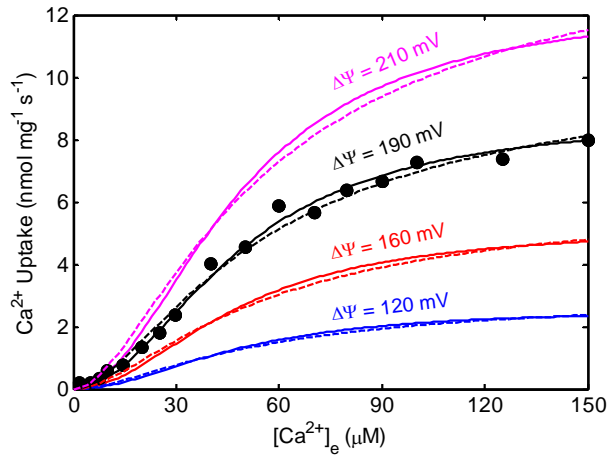


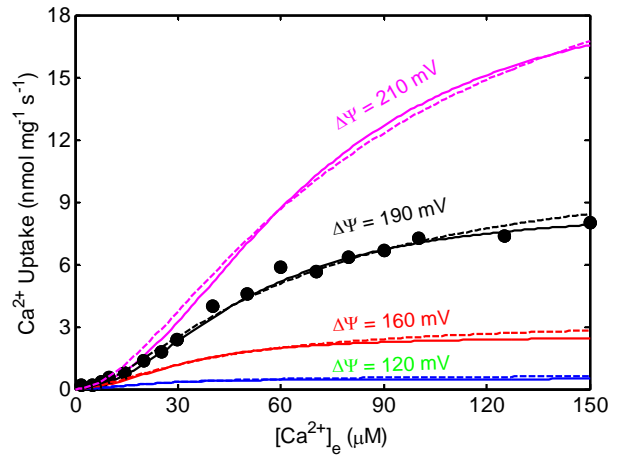
Figure 2: Free-energy barrier formalism for Ca^{2+} transport into mitochondria via the Ca^{2+} uniporter. A(I-III) Consecutive states of the Ca^{2+} -bound uniporter functional unit in the process of Ca^{2+} translocation that is used to derive the dependence of the rate of Ca^{2+} transport on the electrostatic membrane potential $\Delta\Psi$. Here, α_e is the ratio of the potential difference between Ca^{2+} bound at the site of uniporter facing the external side of the IMM and Ca^{2+} in the bulk phase to the total membrane potential $\Delta\Psi$, α_x is the ratio of the potential difference between Ca^{2+} bound at the site of uniporter facing the internal side of the IMM and Ca^{2+} in the bulk phase to the total membrane potential $\Delta\Psi$, β_e is the displacement of external Ca^{2+} from the coordinate of maximum potential barrier, and β_x is the displacement of internal Ca^{2+} from the coordinate of maximum potential barrier. (B) The potential energy barrier profile along the reaction coordinate that is used to derive the dependence of the rate of Ca^{2+} transport on the electrostatic membrane potential $\Delta\Psi$. The dashed line shows the profile of the potential created by the electric field of the charged membrane. The points I, II, and III correspond to the Ca^{2+} -bound uniporter states depicted in the upper panel (A). The rate constants k_{in} and k_{out} are related to the changes in potential energy (Gibbs free-energy) ΔG_{in} and ΔG_{out} . Note that in the absence of electric field ($\Delta\Psi = 0$ mV), the heights of the free-energy barriers in the forward and reverse directions are equal when the dissociation constants for the binding of the uniporter to the external and internal Ca^{2+} are equal: that is, $\Delta G_{in}^0 = \Delta G_{out}^0 = \Delta G^0$ if and only if $K_e^0 = K_x^0 = K^0$.

Fits to Data

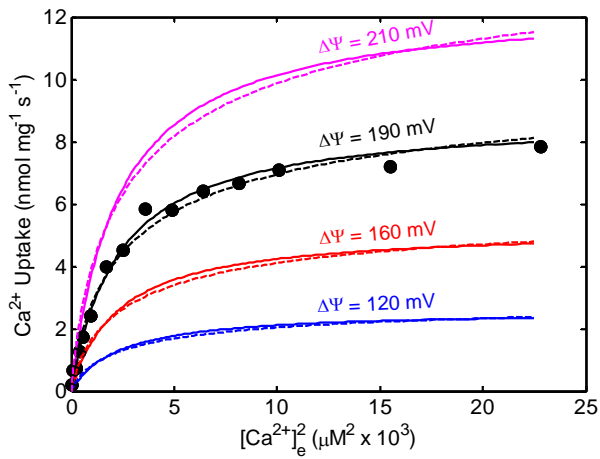
A



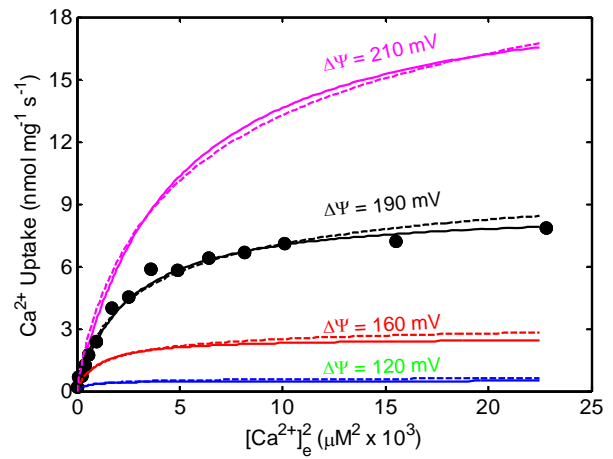
B



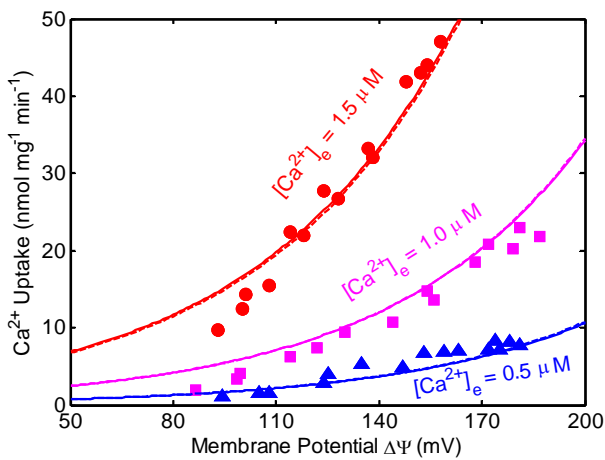
C



D



E



F

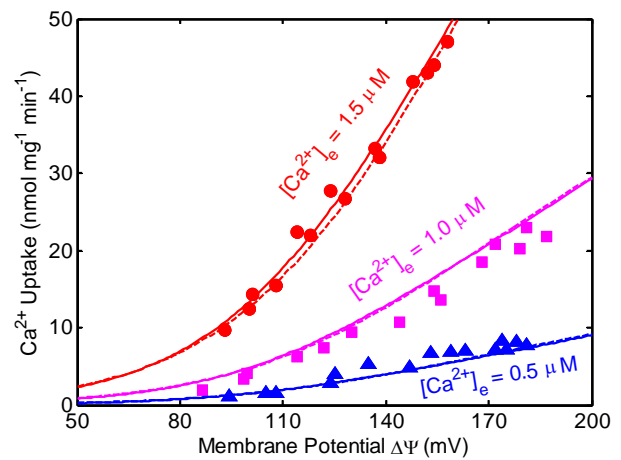


Figure 3: Fitting of Ca^{2+} uniporter model (lines) to data (points) on Ca^{2+} uptake in purified rat liver mitochondria for two different models under two different assumptions. (Upper and middle panels: A-D) The fittings of four different kinetic models of the Ca^{2+} uniporter to the kinetic data of Vinogradov and Scarpa [1] in which the initial rates of Ca^{2+} uptake (points) were measured in respiring mitochondria purified from rat liver with varying levels of extra-mitochondrial buffer Ca^{2+} . Also shown are the model-simulated mitochondrial Ca^{2+} uptake at four different levels of membrane potential $\Delta\Psi$ (lines) in which the models were fitted to the data with $\Delta\Psi = 190$ mV (states 2 and 4 membrane potential). The plots in the upper panels (A,B) differ from the plots in the middle panels (C,D) through the labeling of the x-axis. (Lower panels: E,F) The fittings of the same four kinetic models to the kinetic data of Gunter and coworkers [2,3] in which the initial rates of Ca^{2+} uptake in respiring mitochondria purified from rat liver were measured with varying membrane potential $\Delta\Psi$ for three different levels of extra-mitochondrial buffer Ca^{2+} . To fit the models to these additional data sets, only the uniporter activity parameter (X_{Uni}) is readjusted, while keeping the other kinetic parameter fixed at values as estimated from the fittings in plots (A-D) (see Table 1). The solid lines are the simulations from Model-1 ($K_{1,e} \gg 1$, $K_{1,x} \gg 1$, $K_{2,e} \ll 1$ and $K_{2,x} \ll 1$, such that $K_{1,e} \cdot K_{2,e} = K_e^2$ and $K_{1,x} \cdot K_{2,x} = K_x^2$ are finite), while the dashed lines are the simulations from Model-2 ($K_{1,e} = K_{2,e} = K_e$ and $K_{1,x} = K_{2,x} = K_x$); the left panels (A,C,E) correspond to the fittings and simulations with the assumption that $K_e^0 = K_x^0 = K^0$, while the right panels (B,D,F) correspond to the fittings and simulations with the assumption that K_e^0 and K_x^0 are distinct.

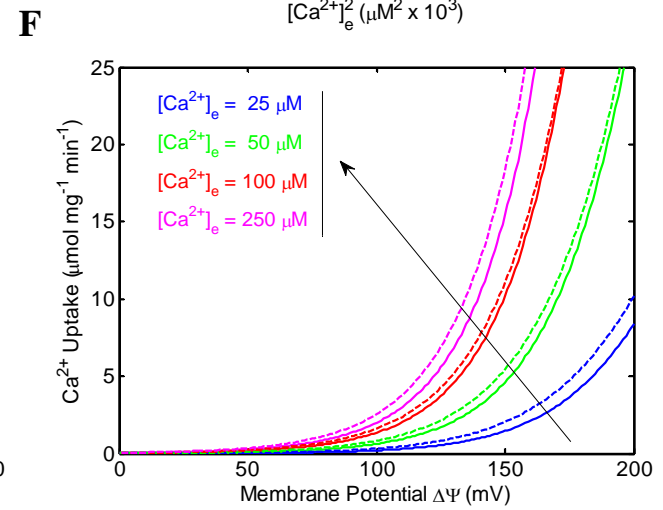
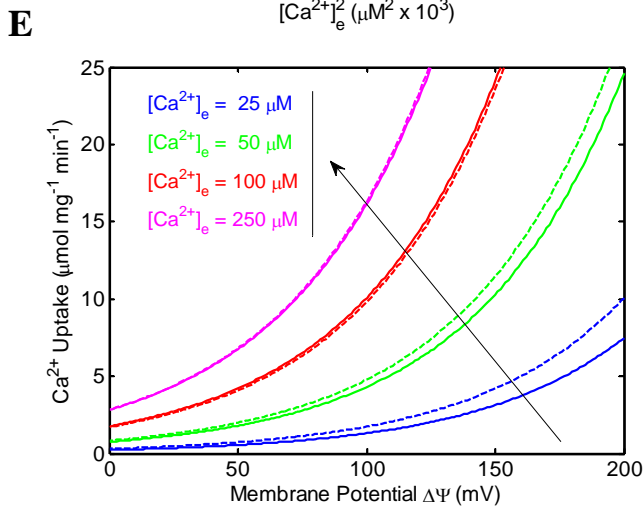
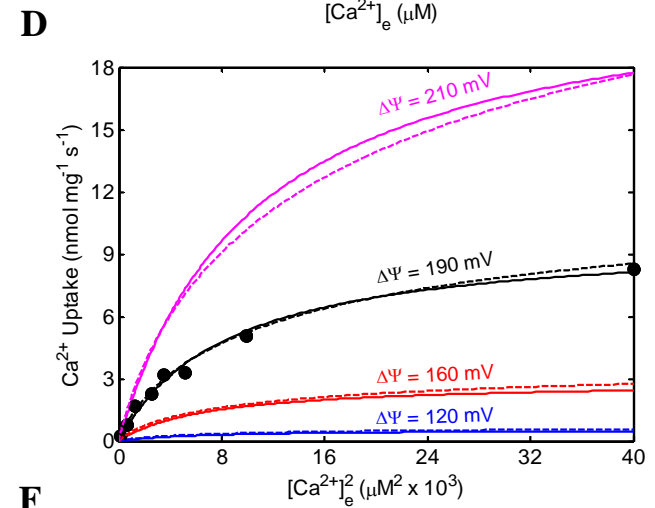
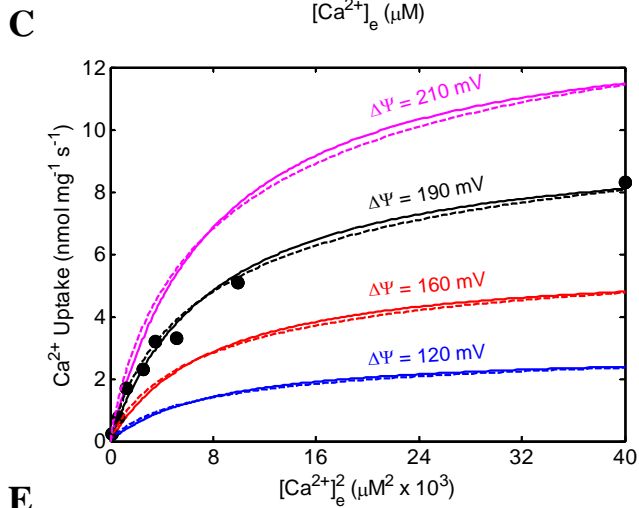
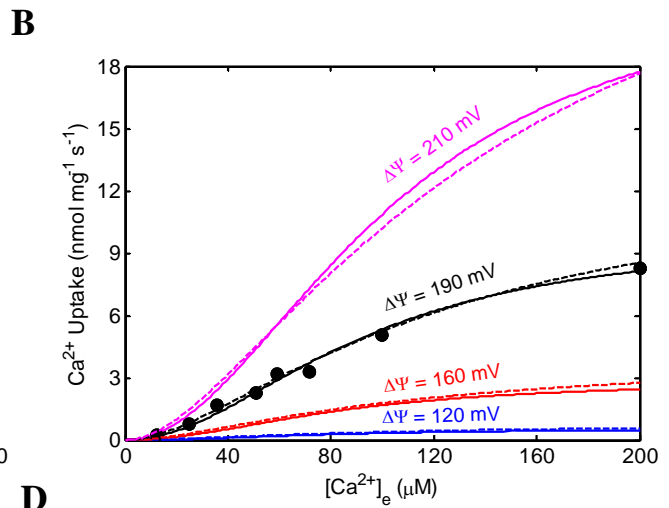
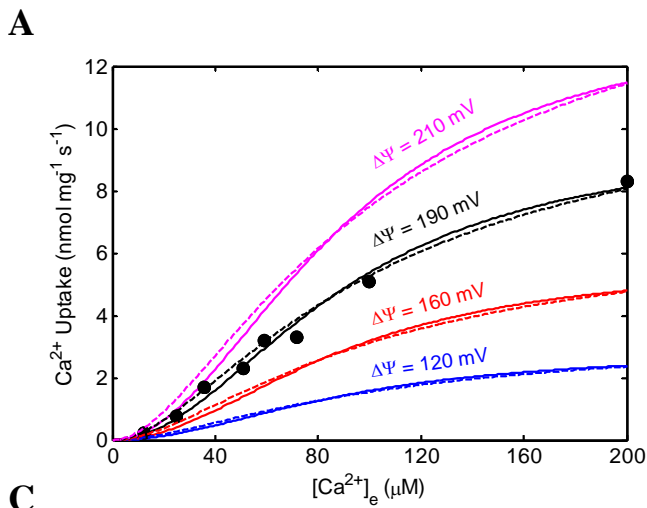


Figure 4: Fitting of Ca^{2+} uniporter model (lines) to data (points) on Ca^{2+} uptake in isolated rat heart mitochondria for two different models under two different assumptions. (Upper and middle panels: A-D) The fittings of four different kinetic models of the Ca^{2+} uniporter to the kinetic data of Scarpa and Graziotti [4] in which the initial rates of Ca^{2+} uptake (points) were measured in respiring mitochondria isolated from rat heart with varying levels of extra-mitochondrial buffer Ca^{2+} . Also shown are the model-simulated mitochondrial Ca^{2+} uptake at four different levels of membrane potential $\Delta\Psi$ (lines) in which the models were fitted to the data with $\Delta\Psi = 190$ mV (states 2 and 4 membrane potential). The plots in the upper panels (A,B) differ from the plots in the middle panels (C,D) through the labeling of the x-axis. To fit the models to these additional data sets from rat heart mitochondria, only the kinetic parameters X_{Uni} , K_e^0 and K_x^0 were readjusted, while keeping the other kinetic parameter α_e , α_x , β_e and β_x fixed at values as estimated from the fittings in Figure 1 for rat liver mitochondria (see Table 1). (Lower panels: E,F) The model-simulated Ca^{2+} uptake in respiring mitochondria isolated from rat heart as a function of membrane potential $\Delta\Psi$ for four different levels of extra-mitochondrial buffer Ca^{2+} (relatively higher levels of buffer Ca^{2+} than those shown in Figure 3 (E,F) for rat liver mitochondria; corresponding to the experimental protocol of Kirichok et al. [5]). For these simulations, the uniporter activity parameter (X_{Uni}) is increased by 150 times, while keeping the other kinetic parameters fixed at values as estimated from the fittings in plots (A-D) (see Table 1). The solid lines are the simulations from Model-1, while the dashed lines are the simulations from Model-2; the left panels (A,C,E) correspond to the fittings and simulations with the assumption that $K_e^0 = K_x^0 = K^0$, while the right panels (B,D,F) correspond to the fittings and simulations with the assumption that K_e^0 and K_x^0 are distinct; model specifications are as mentioned in Figure 3.

References

1. Vinogradov, A., and A. Scarpa. 1973. The initial velocities of calcium uptake by rat liver mitochondria. *J Biol Chem* 248(15):5527-5531.
2. Gunter, T.E., and D.R. Pfeiffer. 1990. Mechanisms by which mitochondria transport calcium. *Am J Physiol* 258(5 Pt 1):C755-786.
3. Wingrove, D.E., J.M. Amatruda, and T.E. Gunter. 1984. Glucagon effects on the membrane potential and calcium uptake rate of rat liver mitochondria. *J Biol Chem* 259(15):9390-9394.
4. Scarpa, A., and P. Graziotti. 1973. Mechanisms for intracellular calcium regulation in heart. I. Stopped-flow measurements of Ca^{2+} uptake by cardiac mitochondria. *J Gen Physiol* 62(6):756-772.
5. Kirichok, Y., G. Krapivinsky, and D.E. Clapham. 2004. The mitochondrial calcium uniporter is a highly selective ion channel. *Nature* 427(6972):360-364.